Sequential exposure and assembly of cyst wall filaments on the surface of encysting *Giardia duodenalis*

R. ARGUELLO-GARCIA[1,2], C. ARGUELLO-LOPEZ[2], A. GONZALEZ-ROBLES[2], A. M. CASTILLO-FIGUEROA[1] *and* M. G. ORTEGA-PIERRES[1]*

[1] *Department of Genetics and Molecular Biology, Centro de Investigación y de Estudios Avanzados-IPN, 07300 Mexico City, D.F., Mexico*
[2] *Department of Experimental Pathology, Centro de Investigación y de Estudios Avanzados-IPN, 07300 Mexico City, D.F., Mexico*

(*Received 5 October 2001; revised 6 March 2002; accepted 25 April 2002*)

SUMMARY

The mode of appearance and assembly of cyst wall filaments on the surface of *Giardia duodenalis* trophozoites committed to encyst was analysed by scanning and transmission electron microscopy (SEM and TEM) and by fluorescence microscopy (FM). SEM showed a progressive appearance of fibril patches, predominantly on the anterior area of ventral and dorsal surfaces, which then spread and coalesced. By TEM, ruthenium red (RR) displayed staining in encysting cells as rodlike spots of variable diameter (3–25 nm), possibly microfibril tips with polyanionic moieties, that displayed tangential associations and random orientations over the cell membrane. In FM assays, the 1,10-phenanthroline derivative of ruthenium red (RR/oPHE) was a specific ligand for these assembling fibrils and this staining was significantly blocked by *N*-acetylgalactosamine (GalNac) and galactosamine (GalN). Interestingly, RR staining was lost when the cyst wall was completely assembled and thickened as observed by TEM and FM. Kinetic FM assays, in which a mAb specific for a 26 kDa *Giardia* cyst wall polypeptide was used concomitantly with RR/oPHE staining, showed a differential pattern for the appearance and reactivity of polypeptide and assembling GalN/GalNac-rich moieties of *Giardia* cyst wall.

Key words: *Giardia duodenalis*, encystation, cyst wall assembly, electron microscopy, fluorescence microscopy.

INTRODUCTION

Biogenesis of a protective cyst wall is a key mechanism for the continuity of infections caused by *Giardia duodenalis*. The cyst wall comprises 2 main components: a double membrane bilayer and a layer of 0·3–0·5 μm which is a complex array of fibrillate material laid down on the outer surface (Erlandsen, Bemrick & Pawley, 1989). The external meshwork involves interconnected filaments of 7–20 nm in diameter that contain peptide and carbohydrate moieties, the polysaccharide component being the most abundant on a molar basis (Manning, Erlandsen & Jarroll, 1992). An important question concerns the form in which these components are expressed on the cell surface during *Giardia* cyst morphogenesis. In this context, Erlandsen *et al*. (1996) used low voltage scanning electron microscopy (LVSEM) combined with immunogold labelling and detected an early deposition of cyst wall material as surface cap-like protrusions that were later embedded in the cyst wall meshwork. Antigenic determinants recognized by polyclonal antibodies were possibly associated with proteins and/or glycoproteins since some discrete cyst components were detected by Western blot assays (Erlandsen *et al*. 1990). However, the detection of carbohydrate-rich moieties and the appearance of the fibrillate layer of *Giardia* cyst wall has not yet been traced in the surface of early encysting cells; thus, the progressive organization of this extracellular matrix has remained unknown. Also, if polysaccharide-rich growing fibrils are to be detected, there is a need to modify conventional fixation protocols in which aldehyde fixatives and osmium tetroxide are used primarily to preserve polypeptide and lipid structures, respectively (Wigglesworth, 1985; Phend, Rustioni & Weinberg, 1995).

Here we report an electron microscopy analysis at scanning (SEM) and transmission (TEM) levels which demonstrates the way in which the polysaccharide-rich, fibrillate material of the cyst wall is laid down and organized in early and late stages of encystation. Kinetic assays of the encystation procedure were performed using fluorescence assays with polypeptide or polysaccharide-specific ligands, in order to determine if the exposure of cyst wall polypeptides on the cell surface and the assembly of cyst wall filaments occurred simultaneously or sequentially in encysting *Giardia*.

* Corresponding author: Departamento de Genética y Biología Molecular, Centro de Investigación y de Estudios Avanzados-IPN, Apartado Postal 14-740 07300 México, D.F., México. Tel: +525 57473800 ext. 5300. Fax: +525 747 7100. E-mail: gortega@lambda.gene.cinvestav.mx

DOI: 10.1017/S0031182002002032 Printed in the United Kingdom

MATERIALS AND METHODS

Parasite cultures

G. duodenalis trophozoites from the WB strain (ATCC no. 30957) were axenically grown at 37 °C in Diamond's TYI-S-33 medium modified by Keister (1983) without bile. Cells were harvested in the log phase after chilling on ice, washed 3 times using cold phosphate-buffered saline, pH 7·2 (PBS), counted in a haemocytometer and adjusted to the required cell number.

In vitro *encystation and cyst purification*

Induction of trophozoites to differentiate was performed by a modification of the method of Schupp *et al*. (1988). Log-phase parasites were inoculated at an initial cell density of 2×10^5 adherent trophozoites/ml in encystation medium (TYI-S-33 plus 5 mg/ml bovine bile adjusted with NaOH to a pH of 7·8). For EM studies, culture tubes were incubated at 37 °C for various time-intervals (3, 6, 9, 12, 15, 18, 21, 24, 42, 66 and 90 h post-inoculation) and cells were harvested and washed as described. Cysts were harvested at the end of the incubation period (90 h) and cellular pellets were treated with an hypotonic shock using double-distilled water overnight at 4 °C. The cell suspension (1–2 ml) was overlaid in 3–5 ml of a 0·85 M sucrose solution. After centrifugation at 750 ***g*** for 10 min, the pellet was resuspended in water and purified cysts were counted and adjusted to the desired concentration in PBS before use.

Scanning electron microscopy (*SEM*)

Samples of fixed parasites (10–25 μl) were placed on 0·5 cm² pieces of Millipore filter (0·22 μm pore) and dehydrated in increasing concentrations of ethanol. After 3 final changes in absolute ethanol for 30 min, the parasites were desiccated with a critical-point drying apparatus (Samdri-780 Tousimis) under CO_2 vapour and covered with gold using a JEOL Fine Coat Ion-Sputter apparatus (JFC-1100). Samples were observed with a JEOL (JMS-35C) scanning EM at 10 kV.

Transmission electron microscopy (*TEM*)

Samples were fixed for 1 h with 2·5 % glutaraldehyde and 1 % paraformaldehyde in cacodylate buffer 0·1 M, pH 7·2, and post-fixed 1 h with 1 % OsO_4 in the same buffer. Parasites were dehydrated under increasing concentrations of ethanol and embedded in Epon 812. Ultrathin sections (50 nm average) were stained with uranyl acetate and lead citrate and observed using a Carl Zeiss EM 10 at 60 kV. When ruthenium red (RR, Polysciences) staining was used, parasites were fixed with 2·5 % glutaraldehyde in cacodylate buffer 0·1 M, pH 7·2, which included the dye at a concentration of 1 mg/ml.

Antigens, antibodies and immunoblot assays

Western blot experiments were performed according to standard methods previously described (Towbin, Staehelin & Gordon, 1979; Ortega-Pierres *et al*. 1988). The monoclonal antibody (5-3C) that recognizes a leucine-rich polypeptide of 26 kDa, named CWP1, located in encystation-specific vesicles (ESVs) and *Giardia* cyst wall (Stibbs, 1989; Mowatt *et al*. 1995), was kindly provided by Henry Stibbs (Tulane University, USA) as culture supernatant. For the preparation of antigenic material, total extracts from trophozoites or cysts were obtained by sonication as previously described (Ortega-Pierres *et al*. 1988) and its chemical modification was carried out by an adaptation of the method reported by Ogier *et al*. (1984). This consisted of the treatment of cyst sonicates (500 μl) with 250 μl of either (a) 200 μg/ml of pronase B (Calbiochem) prepared in 50 mM Tris buffer, pH 7·5, for 4 h at 37 °C, or (b) 30 mM sodium metaperiodate prepared in 50 mM acetate buffer, pH 5·0, overnight at 4 °C in the dark. The mixture was heated at 93 °C for 5 min to inactivate the enzyme and stored at −70 °C until reconstituted in sample buffer (pronase treatment), or dialysed against distilled water at 4 °C then reconstituted in sample buffer and stored at −70 °C until used (periodate treatment). Antigen extract (80 μg/lane) was electrophoretically separated in 5–15 % acrylamide gels (16 × 18 cm) and transferred to nitrocellulose membranes (NCP, Hoefer Scientific Instruments). Supernatants with monoclonal antibody 5-3C were diluted at 1:25 and incubated with NCP strips at 37 °C for 3 h. Goat anti-mouse IgG-HRP conjugate (Sigma) was added at 1:2000 dilution and strips were incubated for 1 h at 37 °C. Antigen–antibody reactions were detected using 4-chloro-1-naphthol (Sigma) as substrate. Equal protein loading of each NCP strip was verified by staining replicates with a solution of 40 % methanol/10 % acetic acid/1 % Amido Black (Sigma).

Fluorescence microscopy (*FM*)

Kinetic analyses were performed on cell samples collected at 0·5 to 2·5 h time-intervals after induction of encystation. In a series of experiments, parasites were washed 3 times in PBS and stained for 5 min at room temperature in a solution of PBS containing a 1,10-phenantroline (Sigma) derivative of RR (RR/oPHE) at a concentration of 10 μg/ml (Bertolesi, De Cidre & Stockert, 1995). Samples were mounted in Vecta-Shield medium (Vector Laboratories) and

https://doi.org/10.1017/S0031182002002032 Published online by Cambridge University Press

observed in a Zeiss epifluorescence photomicroscope model MC 80 fitted with a filter set for violet-blue exciting light (G436, FT510 LP520). Cells displaying a red-orange, punctuate fluorescence on their surface were scored as RR positive. In other experiments, encysting cultures were evaluated by double staining, first using indirect immunofluorescence with the mAb 5-3C then by RR/oPHE staining as described above. For indirect immunofluorescence, PBS-washed cells were incubated for 1 h at 37 °C with mAb 5-3C at a 1:30 dilution in a solution of PBS containing 10% heat-inactivated bovine serum (HyClone). After this, cells were washed 3 times with PBS then incubated for 1 h at room temperature with a 1:100 dilution of fluorescein-conjugated goat anti-mouse IgG (Sigma) in the same diluent used for the first antibody. Cells were again washed with PBS and subjected to RR/oPHE staining as described above. Parasites were observed under white light and under a blue 450–490 FT510 LP520 filter for the green fluorescence associated with mAb 5-3C. Under these conditions RR staining displayed a brilliant red-orange fluorescence. In all cases, at least 300 cells were counted in each sample.

RESULTS

Cyst wall is progressively assembled from microfibril bundles and patches

G. duodenalis cultures displayed a high degree of asynchrony in response to bile components at pH 7·8 as encystation inducing conditions. Cyst numbers increased with the incubation time and up to 50–60% of cells were finally encysted ($3{\cdot}5–4{\cdot}5 \times 10^5$ cysts/ml). More than 75% of cysts were viable as determined by vital staining with fluorescein diacetate and propidium iodide and were infective for Mongolian gerbils (data not shown). SEM was used to analyse cellular morphology and surface topology in differentiating cells. Processing on filter membranes instead of cover-slips yielded a better preservation of the fibrillate material on the surface of these cells. Fibril patches were not an artefact caused by the nitrocellulose matrix since they were not observed in cultures not exposed to encystation inducing conditions (Fig. 1A), their spatial array is mutually distinct and nitrocellulose does not adhere by itself to *Giardia* cell surface. This in turn allowed the observation in detail of a variety of cell surface changes in samples and a sequence of photographic records was collected. In this sequence two criteria were applied (i) cells displaying morphological changes without any modification in their surface (i.e. round, smooth-surfaced cells) were not considered as encysting cells since all the cells showing incipient fibril patches were still pear-shaped, and (ii) only oval, fully capsulated cells were considered as cysts.

In control cultures or cultures harvested after short incubation periods (up to 12 h), pear-shaped trophozoites predominated and their ventral and dorsal surfaces were relatively smooth (Fig. 1A). As a common feature observed in samples of 15–18 h p.i., a proportion of cells (5–15%) underwent the deposition of fibrillate material as irregularly shaped bundles (fibril patches) of variable extension (0·1 μm to > 2 μm) over the dorsal and ventral surfaces (Fig. 1B). In a same cell, incipient patches appeared as small protrusions while other developing patches were significantly greater (Fig. 1C). These disperse patches apparently grew randomly and multiple areas of coalescence, intermeshing and overlapping were progressively seen (Fig. 1D). At this time, the cell surface had a more porous appearance than in non-encysting trophozoites, particularly in the area of the adhesive disk (compare Fig. 1A and D). Flagella were not affected but the rounding up of the parasites (possibly caused by cumulative secretory events at the caudal zone) became apparent (Fig. 1E). As a result of this vectorial growth of the fibrillate meshwork, the fusion of fibril patches apparently advanced from the anterior to the caudal portion of the cells, leading to flagella entrapping (Fig. 1E). Rounded cells completely covered by the filamentous meshwork acquired a 'smooth' texture to their surface and a flagellum-like structure remained later in these populations (Fig. 1F). These cells ('tailed cysts') were still motile. Finally the disappearance of the whole 'tail' from the cell body (Fig. 1G) rendered oval and non-motile cystic forms.

An additional SEM analysis was carried out in samples collected 24 h p.i. and the localization of fibril patches was scored in a total population of 288 cells from which 128 (44%) displayed cyst wall assembly on their surface. Parasites were observed either in dorsal or ventral planes and each plane was divided in anterior and caudal areas, the former being defined by the contour of the adhesive disk. The complete analysis of these images is shown in Table 1. It was noteworthy that a high proportion of cells observed in the ventral plane (86%) displayed fibril assembly over the adhesive disk. Moreover, in 29% of cells fibril patches were observed only over the adhesive disk. Cells observed in the dorsal plane showed similar proportions of fibril patches in anterior and caudal areas (77% and 74% respectively) but 26% of them displayed fibril assembly only over the anterior area. In general, the anterior area in dorsal or ventral plane was the site in which fibril patches were first most frequently observed in encysting parasites (see Fig. 1B).

Most kinetic studies have shown, as in other organisms capable of encysting, that in *Giardia* a decrease in cell proliferation is followed by a higher rate of cell differentiation. Dividing parasites with ESV have been observed by Nomarski optics and a number of non-dividing, non-encysted parasites

https://doi.org/10.1017/S0031182002002032 Published online by Cambridge University Press

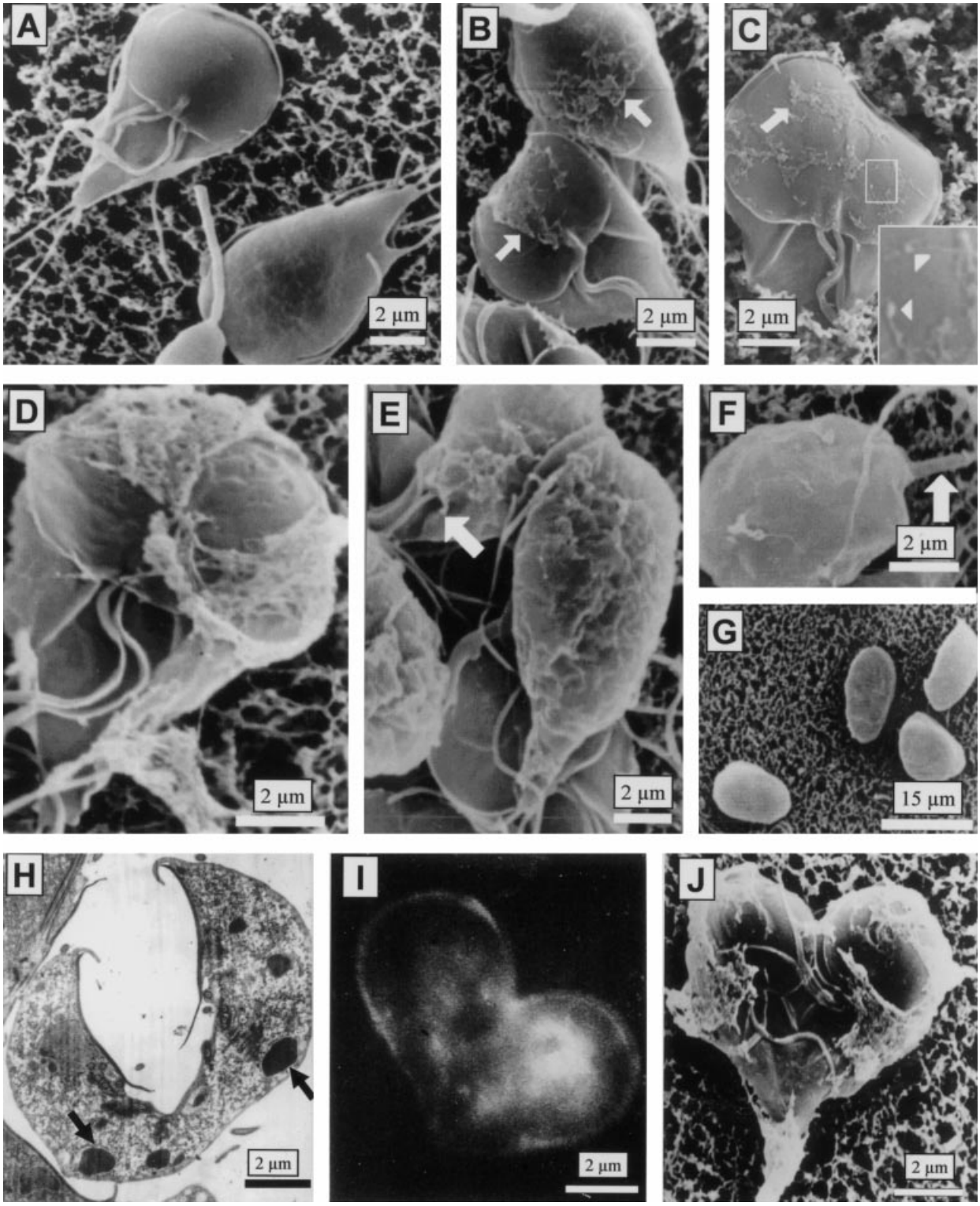

Fig. 1. Detection of early and late wall filament assembly in encysting *Giardia* by SEM (A–G) and intracellular and extracellular phases of encystation displayed by dividing cells (H–J). (A) Dorsal and ventral views of non-induced trophozoites. (B) Fibril bundles (arrows) of varied extension were detected on dorsal and ventral anterior surfaces. (C) Small protrusions (inset, arrowheads) grew as coalescent patches (arrow) in the area over the ventral disk. (D) An encysting cell displaying progressive polymerization of cyst wall matrix in random trajectories. (E) Rounding of the cells was evident as they were completely covered by the fibrous meshwork, and processes of ventral flagella entrapping were seen (arrow). (F) Parasites completely covered with cyst wall components further exhibit a motile 'tail' (arrow) which disappears in mature forms (G). (H) TEM section in which ESVs (arrows) are distributed between daughter cells. (I) FM image of mitotic *Giardia* stained with monoclonal antibody 5-3C. (J) SEM image of cytokinetic forms with concomitant cyst wall assembly. The time sampling (p.i.) was: 9 h in H and I, 12 h in C, 15 h in B and D, 18 h in E, F and J and 24 h in G.

https://doi.org/10.1017/S0031182002002032 Published online by Cambridge University Press

Table 1. Analysis of the distribution of fibril patches in encysting *Giardia* after 24 h of encystation induction ($n = 128$)

Area with fibril patches	Plane	
	Ventral (%)	Dorsal (%)
Anterior	50 (86·2)	54 (77·1)
Caudal	41 (70·7)	52 (74·3)
Anterior and caudal	33 (56·8)	36 (51·4)
Anterior only	17 (29·3)	18 (25·7)
Caudal only	8 (13·8)	16 (22·8)
Total cells	58 (100)	70 (100)

exhibit these structures (Reiner, Douglas & Gillin, 1989). In our study we determined if cyst wall assembly was displayed only by differentiating, non-dividing cells. As expected, some replicative forms exhibited electron-dense ESVs in their cytoplasm that appeared to be equally distributed between the daughter cells (Fig. 1H). However, there were also dividing cells exposing polypeptide, cyst wall-specific material on their surfaces (Fig. 1I) and moreover secreting the filamentous component of the cyst wall (Fig. 1J). This pattern of wall assembly led to fibril intermeshing between cells, thus avoiding the formation of 2 separate cyst walls for the 2 daughter cells.

Assembly of filamentous patches as analysed by RR staining and TEM

The inclusion of RR in the fixing solution was essential in detecting fibril patches by TEM analyses (Fig. 2), i.e. conventional fixation and post-fixation in the absence of RR were ineffective. In this way, RR-positive cells displayed staining as electron-dense spots in defined zones over the cell surface (Fig. 2A). This staining initially highlighted rodlike structures of variable diameter between 3 and 25 nm as observed in cross-sections (Fig. 2A–C). These polyanionic moieties were often layered and showed tangential associations (Fig. 2B). Frequently small spots looked as fused into large spots measuring up to 80 nm. This pattern was consistently observed even in tangential sections of developing cyst walls (Fig. 2C), excluding the possibility that RR could stain microfibrils in longitudinal profiles or sites of microfibril initiation. An unique feature that distinguishes highly structured wall material from that undergoing early assembly can be seen in Fig. 2D. In this situation, developing fibrils had a dense RR staining while cell wall regions with heavily overlapped filaments and close opposition to the cell membrane were RR negative. This phenomenon was progressive since cells displaying a thickening cyst wall are actually losing their ability to be stained by RR (Fig. 2E and F). Thus the filamentous component of the cyst wall, when it reached a mature conformation, presented changes in its polyanionic charge density that no longer allowed RR binding.

Specificity of RR staining

Combination of RR with osmium tetroxide in TEM studies allowed detection of a patchy pattern of staining in encysting parasites. However, this technique did not give a precise value of the proportion of RR-positive cells in samples nor allowed direct determination of the nature of the stained material. In addition, RR is not fluorescent by itself. To overcome these problems, RR was conjugated with 1,10-phenanthroline (RR/oPHE) for staining of encysting cultures and its fluorescence was now detected. RR/oPHE specifically stained encysting parasites in which fibril patches were being assembled (Fig. 3C). When we used the mAb 5-3C, which specifically recognizes a cystic 26 kDa polypeptide (Fig. 3D), a distinct pattern of staining was observed in comparison to RR/oPHE (compare Fig. 3B and C). The apparent blockade of RR/oPHE staining occurred following preincubation of the dye with different sugars including amino- and acetyl-derivatives of hexoses, basically galactose. Cell samples collected to 30 h p.i. were selected because at this time there was a significant proportion of RR/oPHE-positive parasites (13–18% of total cells) in kinetic assays (Fig. 3E). The inclusion of mannose, glucose, galactose, glucosamine and *N*-acetylglucosamine (up to 20 mM) did not reduce these percentages of RR staining. On the other hand, when GalNac (5 mM) was included, the fluorescent staining of parasites was completely abolished. A similar effect was observed with GalN although the inhibition of RR staining required concentrations of 20 mM of the sugar.

Cyst wall filament assembly in encysting cells is preceded by exposure of cyst wall polypeptides

A critical question is whether cyst wall polypeptides and fibril patches are exposed with the same or distinct kinetics on the surface of induced cells. The mAb 5-3C used in these studies clearly recognized polypeptide cyst wall epitopes as judged by immunoblot assays in which pronase B treatment abolished antibody reactivity (Fig. 3D, lane 4) while periodate oxidation was ineffective (Fig. 3D, lane 3). Considering that RR transiently recognizes the GalN/GalNac-rich wall fibrils as observed by FM, double-labelling experiments were performed. In these, induced parasites were incubated with mAb 5-3C and a fluorescein-labelled second antibody, then with RR/oPHE or vice versa.

As shown in Fig. 3E, induced parasites began to display only antibody fluorescence by 5·5 h p.i. This included pear-shaped trophozoites (pre-cysts) and cysts (Fig. 3B), reaching values of more than 50% of

https://doi.org/10.1017/S0031182002002032 Published online by Cambridge University Press

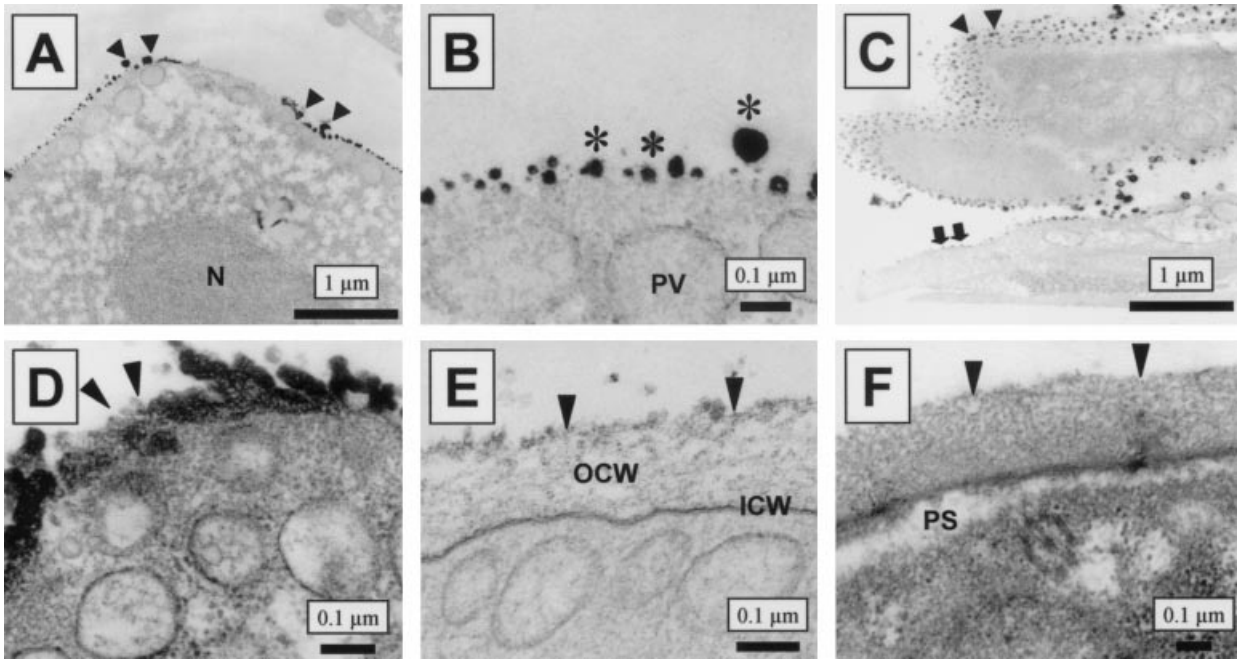

Fig. 2. Detection of extracellular assembly of *Giardia* cyst wall by RR staining. (A) Rodlike structures (spots) of variable diameter, cross-sectioned and RR-stained, as detected on the dorsal surface of a trophozoite (arrowheads). (B) Layered spots in cross-sections are laid down on cell surface and some of them look as fused (*). (C) Cross-section of a trophozoite with RR spots on dorsal surface (lower cell, arrows) and a tangential section of a polymerizing cyst wall with oblique profiles of RR-positive structures (upper cell, arrowheads). (D) An encysting cell with polymerizing cyst wall in a later stage. Profuse overlapping and layering of RR spots is being progressively lost when fibrillate material is appearing (arrowheads). (E) A cross-section of a cyst wall showing the fibrillate outer layer (OCW, arrowheads) which is assembled over the inner membranous layer (ICW) and is no longer stained by RR. (F) After complete wall assembly, the peritropic space (PS) is formed and no RR staining is observed. The time sampling (p.i.) was: 15 h in A and B, 18 h in C and D, 21 h in E and 24 h in F. N, Nucleus; PV, peripheral vacuole.

the total cells by 70 h. RR/oPHE-stained cells were initially observed by 9–10 h p.i. but unlike mAb 5-3C, after reaching peak values of 15–19 % of the total cells between 30 and 50 h p.i., stained parasites were no longer observed after 65 h p.i. Moreover, we never observed pear-shaped trophozoites displaying RR/oPHE fluorescence without antibody reactivity and oval cystic cells were generally negative for RR/oPHE staining (Fig. 3C). This suggests that polypeptide exposure on the cell surface always preceded fibril patch assembly and this assembly was completed in parasites which were previously positive for RR/oPHE. However, not all cells that were positive for monoclonal antibody 5-3C successfully encysted.

DISCUSSION

We showed that cyst wall formation in *G. duodenalis* involves a stepwise pattern. Cyst wall filament assembly is preceded by the biogenesis of intracellular reservoirs such as ESVs in Golgi-like cisternae which transport cyst wall polypeptides to the cell surface (Reiner *et al*. 1989; Reiner, McCaffery & Gillin, 1990). SEM suggested that the cyst wall assembles from separate bundles and patches of fibrils which grow, intercalate and overlap forming the intricate cyst wall.

Using nitrocellulose membranes and RR staining improved preservation of previously unnoticed growing microfibrils in early encysting *Giardia*. SEM results were better when adsorbing and fixing parasites on filter matrix, since dehydration, washing and desiccation were less abrasive upon labile fibril bundles. In TEM analyses, RR had a 2-fold advantage: first, its 1·13 nm diameter prevents crossing intact membranes and therefore in non-permeabilized cells stains only surface structures (Luft, 1971*a*, *b*; 1976); secondly, RR may be complexed with carboxyl or hydroxyl groups of microfibril polysaccharide of developing *Giardia* cyst walls in the presence of osmium tetroxide, producing electron-dense precipitates (Luft, 1971*a*; Murano *et al*. 1990; Fassel & Edminston, 1999). Several filamentous extracellular materials can be fixed by RR such as charged polymers including pectins, mucins and other hexosamine-containing polysaccharides that are not readily seen with conventional EM procedures (Luft, 1971*a*; Szubinska & Luft, 1971; Popov & Ignatovich, 1976; Handley, Hargreaves & Harty, 1988; Murano *et al*. 1990; Oyston & Handley, 1990).

Unlike aforementioned anionic polymers, assembly filaments in encysting *Giardia* were stained by RR only as layered and overlapped rounded spots, while longitudinal profiles of fibrils were not stained

https://doi.org/10.1017/S0031182002002032 Published online by Cambridge University Press

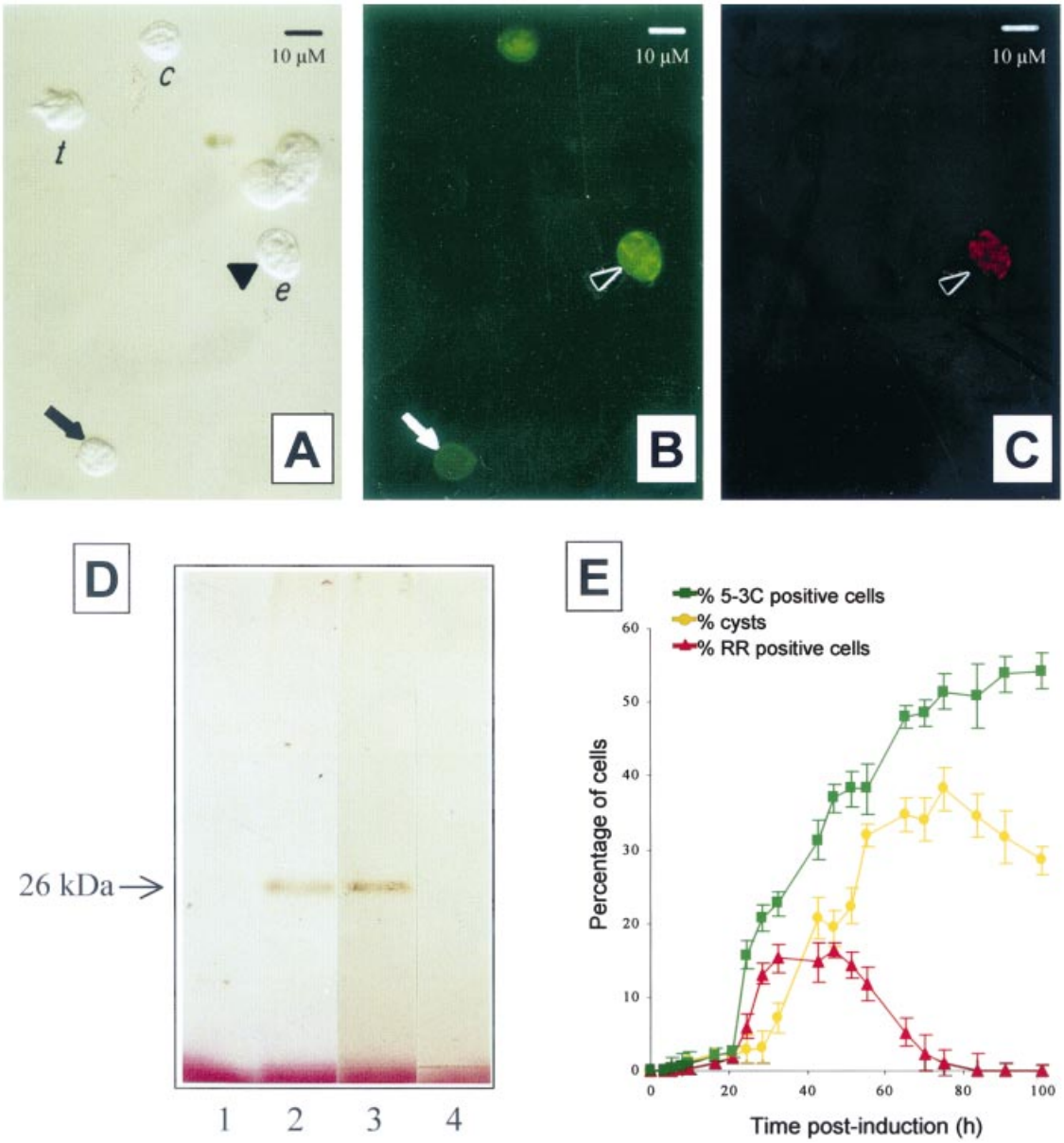

Fig. 3. Selectivity of cyst wall markers and kinetic analysis of its reactivity in encysting cultures. (A) Parasites in different stages of differentiation: trophozoite (*t*), encysting cell (*e*, arrowhead), cyst (*c*) and a pre-cyst (arrow). (B) All these cells except trophozoites are positive for antibody 5-3C staining, and (C) only encysting cell shows reactivity with RR/oPHE. (D) Reactivity of antibody 5-3C tested by Western blot assays. Untreated trophozoite (lane 1) or cyst (lane 2) total antigens were incubated with intact antibody; cyst antigen was then treated with sodium metaperiodate (lane 3) or with pronase (lane 4) and overlaid with intact antibody. (E) Percentages of cells induced to encyst and harvested at different time-intervals that react with antibody 5-3C (green) or RR/oPHE (red), and counts of water-resistant cysts (yellow). Each point corresponds to the mean ± S.D. obtained from 3 independent experiments.

and fully assembled walls did not show reactivity. A similar disappearance of RR staining has been found in rat uterine epithelium during oestrus (Hurtado de Mendoza, Moreno & López-Campos, 1985). A likely explanation for these staining patterns is that only fibril tips under active growth i.e. polymer ends able to intermesh and coalesce, exhibit polyanionic moieties accessible to RR binding. This could be supported by a GalNac/GalN-rich polymer that by itself is non-osmiophilic and has a scarce charge density. These factors are consistent with known interactions of osmium tetroxide and RR in EM (Hayat, 1970; Fassel & Edminston, 1999). The polymerizing wall saccharide may interact with pre-existing cyst wall polypeptides that are later embedded within the mature filaments (Erlandsen *et al.* 1990, 1996). Indeed, antibodies against cyst wall polypeptides interfere with cyst wall formation (Campbell & Faubert, 1994). Thus cyst wall polymerization may cause changes in the exposure of chemical groups as polypeptides and saccharides co-polymerize. This might explain why certain lectins with putative specificity for GalNac (*Phaseolus limensis*) react with *Giardia* cyst wall (Jarroll *et al.*

https://doi.org/10.1017/S0031182002002032 Published online by Cambridge University Press

1989) while others of similar selectivity (phytohemagglutinin, *Dolichos biflorus* and *Helix pomatia*) do not (Ward *et al*. 1985).

Specificity assays for RR/oPHE suggested a GalN/GalNac-richness of *Giardia* fibril patches or cyst wall filaments. Likewise, cyst fibrous material retains its morphological characteristics after boiling in SDS, despite releasing proteins and glycoproteins by reductive agents (McCaffery, Faubert & Gillin, 1994). Other studies on intact cysts and SDS-insoluble cyst walls by Jarroll *et al*. (1989) suggested that GalN and GalNac were major cyst wall components, which was confirmed later in amyloglycosidase and proteinase-treated cyst walls (Manning *et al*. 1992). Solubilized filaments were further analysed and found to consist of a [D-GalNAc ($\beta 1 \rightarrow 3$)-D-GalNAc]$_n$ homopolymer (Jarroll *et al*. 2001). We confirm, *in situ*, that GalN/GalNac contained in the filamentous structure of *G. duodenalis* cyst wall might contribute to the physicochemical resistance of this one.

The cyst wall assembly shown here encompasses early steps of precursors laid down in the surface as fibril bundles that spread and coalesce in anterior and caudal areas of encysting parasites. This pattern is similar in assembling microfibrils of ($\beta 1 \rightarrow 3$)-glucan of regenerating *Candida albicans* protoplasts (Osumi, 1998). Tangential associations among polyanionic moieties in developing fibrils may explain the layering or vertical spreading of this meshwork and are reminiscent of intermicrofibrillar hydrogen bonding found in cellulose bundles in *Acetobacter xylinum* (Brown, Willison & Richardson, 1976). A role for the *Giardia* cytoskeleton on wall fibril orientation may be inferred considering that the colchicine-resistant clone WBC7, defective in cyst production, yields a high proportion of cysts with anomalously assembled walls (R. Argüello-García *et al*., unpublished observations). Also, fibril associations and a possible process of end synthesis (tip growth) in assembling *Giardia* cyst wall, like during cellulose or chitin fibril development (Bracker, Ruiz-Herrera & Bartnicki-Garcia, 1976; Brown, 1985), agree with the coalescence among multiple fibril patches and with cyst clustering under static encystation (Erlandsen *et al*. 1996). The localization of a catalytic complex responsible for wall filament growth, whether membrane-bound, fibril tip-associated or vesicle-contained, will require synthase-specific probes. Only a chitin synthase-like activity has been proposed for *Giardia* encystation (Gillin *et al*. 1987) and other potentially related transferase activities: a particulate UDP-GlcNac, a soluble UDP-GalNac and a particulate β-1,3-GalNAc increased in encysting parasites (Das & Gillin, 1996; Karr *et al*. 1994; Jarroll *et al*. 2000).

Further, we observed 3 unique features during early and late cyst wall assembly. The first involves flagella entrapping, where caudal flagella coated by wall filaments are retracted, immobilizing encysting cells, and the cyst 'tail' disappears at late stages. Flagella entrapping and retraction was suggested by Erlandsen *et al*. (1996), but using anti-tubulin and anti-cyst antibodies we observed that isolated 'tails' contain only cyst wall components, suggesting that these 'tails' are excised from cell body. Secondly, no rounded *pre-cyst* stages were observed in *Giardia* encystation unlike other protozoa such as *Blastocystis hominis* (Suresh *et al*. 1994) and *Entamoeba invadens* (Avron *et al*. 1983). In *G. duodenalis*, rounding coincided with secretory events related to wall assembly; therefore, *Giardia* pre-cysts present cytoplasmic ESVs and cyst surface antigens but cyst wall filament assembly or cytokinesis are *not* yet performed. Thirdly, some dividing cells displayed wall filament assembly. We hypothesize that during culture, encysting efficiency is greater when the growth rate decreases, being unlikely that daughter cells become mature cysts. However, some cells might complete both cytokinesis and differentiation since M phase in the trophozoite's cycle ($\sim$ 30 min) is shorter than that required for extracellular assembly of *Giardia* cyst walls *in vitro* (5–6 h) (R. Argüello-García *et al*., unpublished observations).

Using fluorescent tracers to detect early filament assembly and cyst wall polypeptides in encysting cells, provided us important insights about extracellular encystation. Thus, cell wall matrix completes assembly only when polypeptides are on the surface, likely serving as a *template* for filament growth and assembly. Though surface cyst antigens detected by antibodies (Gillin *et al*. 1987; Sterling *et al*. 1988; Stibbs, 1989; Erlandsen *et al*. 1990, 1996; Ward *et al*. 1990; Gillin, Reiner & McCaffery, 1991; Campbell & Faubert, 1994; Lujan *et al*. 1995*a*; Mowatt *et al*. 1995) are not definitive criteria of full assembly of *Giardia* cyst walls, they may help pre-cyst characterization. Thus, the role of polypeptides in wall assembly has not been clarified even when they are uniformly embedded within filaments of variable diameter (Erlandsen *et al*. 1996). Two structurally related cyst wall proteins of intracellular trafficking within ESVs, namely CWP1 (recognized by mAb 5-3C) and CWP2, have been described and the sequences of their corresponding genes have been reported (Mowatt *et al*. 1995; Lujan *et al*. 1995*a*). Moreover, compelling evidence on the vesicular trafficking and targeting to cyst wall of CWP1 has been obtained with the use of CWP1-green fluorescent protein chimeras (Hehl, Marti & Köhler, 2000). CWPs belong to the small leucine-rich proteoglycan family (SLRP) and contain leucine-rich domains flanked by cysteine clusters (Lujan *et al*. 1995*a*; Hockling, Shinomura & McQuillan, 1998). Cysteine-rich motifs might participate in protein multimer formation on cell surfaces by disulfide cross-linking as occurs in fibronectin assembly (McDonald, 1988), whereas

leucine-rich domains provide flexibility for protein–protein or protein–saccharide interactions (Lujan *et al*. 1995*a*; Hocking *et al*. 1998). These interactions may contribute to tangential interfibrillar associations, fibril overlapping and the orientation of wall filaments.

It has been suggested that CWPs may not be glycosylated when intracellular, only when exposed on the surface (Mowatt *et al*. 1995; Lujan *et al*. 1995*a*). Polymerization of GalN/GalNac-rich fibrils might intercalate polypeptides and promote their final co-assembly as *glycoproteins* since: (a) at least some proteins and glycoproteins can be removed from purified cyst walls by disulfide-bridge breaking (Das & Gillin, 1996; McCaffery *et al*. 1994), (b) serine and threonine residues in CWP1 and CWP2 are potential *O*-glycosylation sites (Mowatt *et al*. 1995; Lujan *et al*. 1995*a*), (c) GalNac transferase activities have been detected in encysting trophozoites at times longer than required for CWP biosynthesis (Macechko *et al*. 1992; Lujan *et al*. 1995*a*, *b*) (d) GalN/GlcN incorporation by pUDP-GT yields proteinase-sensitive products (Das & Gillin, 1996), and (e) the altered electrophoretic mobility of CWPs at late times of encystation (12–24 h) (Fig. 3 of Lujan *et al*. 1995*a*).

In conclusion, we provide new data on how *Giardia* cyst wall filaments are extracellularly assembled in early and late stages of cyst biogenesis. Unravelling the biomolecular mechanisms of wall assembly will identify critical points during encystation, perhaps to interfere with the parasite's life-cycle and to block its transmission.

The authors are grateful to Derek Wakelin, Jacqueline Upcroft and Leopoldo Flores Romo for critically reading this manuscript. We thank Sirenia González Pozos and María de Lourdes Rojas (UME-Cinvestav), María Magdalena Miranda Sánchez and Juana Calderón Amador for their excellent technical support; René López Bolaños and Blanca Herrera for technical assistance, and Arturo Pérez Taylor-Reyes for part of the art work. The authors wish to dedicate this work to the memory of Dr Carlos Argüello-López (1946–1997) for his invaluable scientific contributions. This work was supported by grants from CONACyT-Mexico (ref. M-9309-3391 and 29489M).

REFERENCES

AVRON, B., BRACHA, R., DEUTSCH, M. R. & MIRELMAN, D. (1983). *Entamoeba invadens* and *Entamoeba histolytica*: Separation and purification of precysts and cysts by centrifugation on discontinuous density gradients of percoll. *Experimental Parasitology* **55**, 265–269.

BERTOLESI, G. E., DE CIDRE, L. L. & STOCKERT, J. C. (1995). Formation and microscopical application of a fluorescent 1,10-phenantroline derivative of ruthenium red. *Acta Histochemica* **97**, 401–408.

BRACKER, C. E., RUIZ-HERRERA, J. & BARTNICKI-GARCIA, S. (1976). Structure and transformation of chitin synthetase particles (chitosomes) during microfibril synthesis *in vitro*. *Proceedings of the National Academy of Sciences*, *USA* **73**, 4570–4574.

BROWN, R. M. JR. (1985). Cellulose microfibril assembly and orientation: recent developments. *Journal of Cell Science* (Suppl.) **2**, 13–32.

BROWN, R. M. JR., WILLISON, J. H. M. & RICHARDSON, C. L. (1976). Cellulose biosynthesis in *Acetobacter xylinum*: Visualisation of the site of synthesis and direct measurement of the *in vitro* process. *Proceedings of the National Academy of Sciences*, *USA* **73**, 4565–4569.

CAMPBELL, J. D. & FAUBERT, G. M. (1994). Recognition of *Giardia lamblia* cyst-specific antigens by monoclonal antibodies. *Parasite Immunology* **16**, 211–219.

DAS, S. & GILLIN, F. D. (1996). *Giardia lamblia*: increased UDP-*N*-acetyl-D-glucosamine and *N*-acetyl-D-galactosamine transferase activities during encystation. *Experimental Parasitology* **83**, 19–29.

ERLANDSEN, S. L., BEMRICK, W. J. & PAWLEY, J. (1989). High-resolution electron microscopy evidence for the filamentous structure of the cyst wall in *Giardia muris* and *Giardia duodenalis*. *Journal of Parasitology* **75**, 787–797.

ERLANDSEN, S. L., BEMRICK, W. J., SCHUPP, D. E., SHIELDS, J. M., JARROLL, E. L., SAUCH, J. E. & PAWLEY, J. B. (1990). High-resolution immunogold localization of *Giardia* cyst wall antigens using field emission SEM with secondary and backscatter electron imaging. *Journal of Histochemistry and Cytochemistry* **38**, 625–632.

ERLANDSEN, S. E., MACECHKO, P. T., VAN KEULEN, H. & JARROLL, E. L. (1996). Formation of the *Giardia* cyst wall: studies on extracellular assembly using immunogold labeling and high resolution field emission SEM. *Journal of Eukaryotic Microbiology* **43**, 416–429.

FASSEL, T. A. & EDMINSTON, C. E. (1999). Ruthenium red and the bacterial glycocalyx. *Biotechnic and Histochemistry* **74**, 194–212.

GILLIN, F. D., REINER, D. S., GAULT, M. J., DOUGLAS, H., DAS, S., WUNDERLICH, A. & SAUCH, J. F. (1987). Encystation and expression of cyst antigens by *Giardia lamblia* in vitro. *Science* **235**, 1040–1043.

GILLIN, F. D., REINER, D. S. & MCCAFFERY, M. (1991). Organelles of protein transport in *Giardia lamblia*. *Parasitology Today* **7**, 113–116.

HANDLEY, P. S., HARGREAVES, J. & HARTY, D. W. S. (1988). Ruthenium red staining reveals surface fibrils and a layer external to the cell wall of *Streptococcus salivarius* HB and adhesion deficient mutants. *Journal of General Microbiology* **134**, 3165–3172.

HAYAT, M. A. (1970). *Principles and Techniques of Electron Microscopy : Biological Applications*, *Vol. 1*, pp. 163–164. Van Nostrand Reinhold Company, New York.

HEHL, A. B., MARTI, M. & KÖHLER, P. (2000). Stage-specific expression and targeting of cyst wall protein-green fluorescent protein chimeras in *Giardia*. *Molecular Biology of the Cell* **11**, 1789–1800.

HOCKING, A. M., SHINOMURA, T. & MCQUILLAN, D. J. (1998). Leucine-rich repeat glycoproteins of the extracellular matrix. *Matrix Biology* **17**, 1–19.

HURTADO DE MENDOZA, M. V., MORENO, F. J. & LOPEZ-CAMPOS, J. L. (1985). Permeability and changes in

carbohydrate moiety in rat endometrial epithelium during oestrus as revealed by ruthenium red. *Biology of the Cell* **53**, 187–190.

JARROLL, E. L., MANNING, P., LINDMARK, D. G., COGINS, J. R. & ERLANDSEN, S. L. (1989). *Giardia* specific cyst wall carbohydrate: evidence for the presence of galactosamine. *Molecular and Biochemical Parasitology* **32**, 121–132.

JARROLL, E. L., MACECHKO, P. T., STEIMLE, P. A., BULIK, D., KARR, C. D., VAN KEULEN, H., PAGET, T. A., GERWIG, G., KAMERLING, J., VLIEGENTHART, J. & ERLANDSEN, S. (2001). Regulation of carbohydrate metabolism during *Giardia* encystment. *Journal of Eukaryotic Microbiology* **48**, 22–26.

KEISTER, D. B. (1983). Axenic culture of *Giardia lamblia* in TYI-S-33 medium supplemented with bile. *Transactions of the Royal Society of Tropical Medicine and Hygiene* **72**, 431–432.

LUFT, J. H. (1971*a*). Ruthenium red and violet. I. Chemistry, purification, methods of use for electron microscopy and mechanism of action. *Anatomical Record* **171**, 347–368.

LUFT, J. H. (1971*b*). Ruthenium red and violet. II. Fine structural localisation in animal tissues. *Anatomical Record* **171**, 369–416.

LUFT, J. H. (1976). The structure and properties of cell surface coat. *International Reviews in Cytology* **45**, 291–370.

LUJAN, H. D., MOWATT, M. R., CONRAD, J. T., BOWERS, B. & NASH, T. E. (1995*a*). Identification of a novel *Giardia lamblia* cyst wall protein with leucine-rich repeats. *Journal of Biological Chemistry* **270**, 29307–29313.

LUJAN, D., MAROTTA, A., MOWATT, M. R., SCIAKY, N., LIPPINCOTT-SCHWARTZ, J. & NASH, T. E. (1995*b*). Developmental induction of golgi structure and function in the primitive eukaryote *Giardia lamblia*. *Journal of Biological Chemistry* **270**, 4612–4618.

MACECHKO, P. T., STEIMLE, P. A., LINDMARCK, D. G., ERLANDSEN, S. L. E. & JARROLL, E. L. (1992). Galactosamine-synthesizing enzymes are induced when *Giardia* encysts. *Molecular and Biochemical Parasitology* **56**, 301–310.

MANNING, P., ERLANDSEN, S. L. E. & JARROLL, E. L. (1992). Carbohydrate and amino acid analyses of *Giardia muris* cysts. *Journal of Protozoology* **39**, 290–296.

MCCAFFERY, J. M., FAUBERT, G. M. & GILLIN, F. D. (1994). *Giardia lamblia*: traffic of a trophozoite variant surface protein and a major cyst wall epitope during growth, encystation, and antigenic switching. *Experimental Parasitology* **79**, 236–249.

MCDONALD, J. A. (1988). Extracellular matrix assembly. *Annual Reviews in Cell Biology* **4**, 183–207.

MOWATT, M. R., LUJAN, H. D., COTTEN, D. B., BOWERS, B., YEE, J., NASH, T. E. & STIBBS, H. H. (1995). Developmentally regulated expression of a *Giardia lamblia* cyst wall protein gene. *Molecular Microbiology* **15**, 955–963.

MURANO, E., PAOLETTI, S., CESÀRO, A. & RIZZO, R. (1990). Ruthenium red complexation with ionic polysaccharides in dilute aqueous solutions: chirooptical evidence of stereospecific interaction. *Analytical Biochemistry* **187**, 120–123.

OGIER, J. A., KLEIN, J. P., SOMMER, P. & FRANK, R. M. (1984). Identification and preliminary characterisation of saliva-interacting surface antigens of *Streptococcus mutans* by immunoblotting, ligand blotting, and immunoprecipitation. *Infection and Immunity* **45**, 107–112.

ORTEGA-PIERRES, M. G., LASCURAIN, R., ARGÜELLO-GARCIA, R., CORAL-VAZQUEZ, R., ACOSTA, G. & SANTOS, J. I. (1988). The response of humans to antigens of *Giardia lamblia*. In *Advances in Giardia Research* (ed. Wallis, P. M. & Hammond, B. R.), pp. 177–180. University of Calgary Press, Calgary.

OSUMI, M. (1998). The ultrastructure of yeast: cell wall structure and formation. *Micron* **29**, 207–233.

OYSTON, P. C. F. & HANDLEY, P. S. (1990). Surface structures, haemagglutination and cell surface hydrophobicity of *Bacteroides fragilis* strains. *Journal of General Microbiology* **136**, 941–948.

PHEND, K. D., RUSTIONI, A. & WEINBERG, R. J. (1995). An osmium-free method of epon embedment that preserves both ultrastructure and antigenicity for post-embedding immunocytochemistry. *Journal of Histochemistry and Cytochemistry* **43**, 283–292.

POPOV, V. L. & IGNATOVICH, V. F. (1976). Electron microscopy of surface structures of *Rickettsia prowazeki* stained with ruthenium red. *Acta Virologica* **20**, 424–428.

REINER, D. S., DOUGLAS, H. & GILLIN, F. D. (1989). Identification and localisation of cyst-specific antigens of *Giardia lamblia*. *Infection and Immunity* **57**, 963–968.

REINER, D. S., MCCAFFERY, M. & GILLIN, F. D. (1990). Sorting of cyst wall proteins to a regulated secretory pathway during differentiation of the primitive eukaryote, *Giardia lamblia*. *European Journal of Cell Biology* **53**, 142–153.

SCHUPP, D. G., JANUSCHKA, M. M., SHERLOCK, L. A. F., STIBBS, H. H., MEYER, E. A., BEMRICK, W. J. & ERLANDSEN, E. A. (1988). Production of viable *Giardia* cysts *in vitro*: determination by fluorogenic dye staining, excystation, and animal infectivity in the mouse and Mongolian gerbil. *Gastroenterology* **95**, 1–10.

STERLING, C. R., KUTOB, R. M., GIZINSKI, M. J., VERASTEGUI, M. & STETZENBACH, L. (1988). *Giardia* detection using monoclonal antibodies recognizing determinants of *in vitro* derived cysts. In *Advances in Giardia Research* (ed. Wallis, P. M. & Hammond, B. R.), pp. 219–222. University of Calgary Press, Calgary.

STIBBS, H. H. (1989). Monoclonal antibody-based enzyme immunoassay for *Giardia lamblia* antigen in human stool. *Journal of Clinical Microbiology* **27**, 2582–2588.

SURESH, K., HOWE, J., CHONG, S. Y., NG, G. C., HO, L. C., LOH, A. K., RAMACHANDRAN, N. P., YAP, E. H. & SINGH, M. (1994). Ultrastructural changes during *in vitro* encystment of *Blastocystis hominis*. *Parasitology Research* **80**, 327–335.

SZUBINSKA, B. & LUFT, J. H. (1971). Ruthenium red and violet. III. Fine structure of the plasma membrane and extraneous coats in amoebae (*A. proteus* and *Chaos chaos*). *Anatomical Record* **171**, 417–442.

TOWBIN, H., STAEHELIN, T. & GORDON, J. (1979). Electrophoretic transfer of proteins from polyacrylamide gels to nitro-cellulose sheets: procedure and some applications. *Proceedings of the National Academy of Sciences, USA* **76**, 4350–4354.

WARD, H. D., ALROY, J., LEV, B. I., KEUSCH, G. T. & PEREIRA, M. E. A. (1985). Identification of chitin as a structural component of *Giardia* cysts. *Infection and Immunity* **49**, 629–634.

WARD, H. D., KANE, A. V., ORTEGA-BARRIA, E., KEUSCH, G. T. & PEREIRA, M. E. A. (1990). Identification of developmentally regulated *Giardia lamblia* cyst antigens using GCSA-1, a cyst-specific monoclonal antibody. *Molecular Microbiology* **4**, 2095–2102.

WIGGLESWORTH, V. B. (1985). The distribution of lipid in the cell structure: an improved method for the electron microscope. *Tissue and Cell* **13**, 19–34.

https://doi.org/10.1017/S0031182002002032 Published online by Cambridge University Press